Syntheses, Structures, Photoluminescence, and Theoretical Studies of a Novel Class of d^{10} Metal Complexes of 1*H*-[1,10]phenanthrolin-2-one

Shao-Liang Zheng,[a, b] Jie-Peng Zhang,[a] Xiao-Ming Chen,*[a] Zhen-Li Huang,[c] Zhen-Yang Lin,[d] and Wing-Tak Wong*[b]

Abstract: A novel asymmetric monosubstituted 1,10-phenanthroline, Hophen · 0.5 H_2O (**1**, Hophen = 1*H*-[1,10]phenanthrolin-2-one), was generated by a facile route, and a novel class of crystalline, d^{10}-metal, monomeric or oligomeric complexes of this ligand, namely $[Hg(ophen)_2] \cdot 4H_2O \cdot CH_2Cl_2$ (**2**), $[Cd_3Cl(ophen)_5] \cdot 1.5H_2O \cdot 2CH_2Cl_2$ (**3**), and $[Zn_4O(ophen)_4(OAc)_2] \cdot 4H_2O \cdot 2CH_2Cl_2$ (**4**), were obtained by means of liquid diffusion, and were characterized by X-ray crystallography and photoluminescence studies. Complex **1** exhibits a hydrogen-bonded dimeric structure, **2** is a neutral monomeric complex, **3** has a trinuclear structure with the ophen ligand acting as a bridge through the ketone groups, and **4** features a tetranuclear Zn_4O core that is consolidated further by bridging ophen and acetate ligands. All the complexes display photoluminescent properties in the blue/green region. The photoluminescent mechanisms were investigated by means of molecular orbital calculations, which showed that the photoluminescent properties are ligand-based and can be tuned upon ligation to different metal ions.

Keywords: density functional calculations · d^{10} metal complexes · luminescence · N,O ligands

Introduction

Blue luminescent coordination complexes have been an active research field for decades because of their potential applications in materials science, the most attractive of these is their use as blue emitters in full-color electroluminescent displays.[1–7] However, stable blue luminescent complexes that are useful in electroluminescent devices are still rare and most of them are 8-hydroxyquinoline-, azomethine-, or 7-azaindole-based complexes of Al^{III}, B^{III}, or Zn^{II}.[1–4] Meanwhile, the chemistry of d^{10} metal clusters is of current interest not only on account of their interesting structures but also because of their photoluminescent and/or electroluminescent properties.[4–10] We and others have synthesized a number of such blue photoluminescent polynuclear d^{10} metal complexes featuring novel structures.[4–8] Unfortunately, most of them are involatile so that it is difficult to investigate their electroluminescent properties. We therefore initiated the search for novel ligands that could form sublimable d^{10} metal complexes that exhibit blue luminescence. Recently, we reported a series of copper complexes with a novel 1*H*-[1,10]phenanthrolin-2-one (Hophen) ligand that was synthesized by the hydrothermal treatment of $Cu(NO_3)_2$ and 1,10-phenanthroline in a weakly basic solution.[10] Moreover, it has been found that neutral Cu^{I} complexes of the deprotonated Hophen can be readily vacuum-deposited to form thin films.[11] This observation encouraged us to search for other luminescent d^{10} clusters based on Hophen. We isolated this asymmetric monosubstituted 1,10-phenanthroline ligand that is able to chelate and to bridge metal atoms through two nitrogen sites and an oxygen site. Herein, we describe the syntheses, crystal structures, and photoluminescent properties of Hophen and a novel class of d^{10} metal complexes of this ligand, namely Hophen · 0.5 H_2O (**1**), $[Hg(ophen)_2] \cdot 4H_2O \cdot CH_2Cl_2$ (**2**), $[Cd_3Cl(ophen)_5] \cdot 1.5H_2O \cdot 2CH_2Cl_2$ (**3**), and

[a] Prof. Dr. X.-M. Chen, S.-L. Zheng, J.-P. Zhang
School of Chemistry and Chemical Engineering
Sun Yat-Sen University
Guangzhou 510275 (China)
Fax: (+86) 20-8411-2245
E-mail: cescxm@zsu.edu.cn

[b] Prof. Dr. W.-T. Wong, S.-L. Zheng
Department of Chemistry
The University of Hong Kong
Pokfulam Road
Hong Kong (China)
E-mail: wtwong@hkcc.hku.hk

[c] Z.-L. Huang
State Key Laboratory of Optoelectronic Materials and Technologies
Sun Yat-Sen University
Guangzhou 510275 (China)

[d] Prof. Dr. Z.-Y. Lin
Department of Chemistry
The Hong Kong University of Science and Technology
Clear Water Bay, Kowloon
Hong Kong (China)

Supporting information for this article is available on the WWW under http://www.chemeurj.org/ or from the author

DOI: 10.1002/chem.200304855

$[Zn_4O(ophen)_4(OAc)_2]\cdot 4H_2O\cdot 2CH_2Cl_2$ (**4**), all of which are photoluminescent in the blue/green region. The photoluminescence mechanisms have been studied with molecular orbital (MO) calculations.

Results and Discussion

Synthesis: The neutral, asymmetric, monosubstituted 1,10-phenanthroline Hophen was directly obtained from demetalation of its copper complexes, which were subtly obtained by the hydrothermal treatment of $Cu(NO_3)_2$ and 1,10-phenanthroline.[10] The asymmetric derivatives of 1,10-phenanthroline or 2,2′-bipyridyl are of particular interest for applications in photochemistry,[12, 13] and the synthesis of such asymmetrically substituted compounds is still challenging, although a few examples of general multistep methods that use rigorous reaction conditions are known.[14] In our hydrothermal approach, the presence of copper(II) ions and weakly basic conditions are critical. The coordination of a copper(II) ion may activate the α positions for the nucleophilic attack by hydroxide ions and control the substitution reaction at only one α position of the phenanthroline or bipyridyl ligand.[10, 15] The copper(II) ions also serve as an oxidizing agent to fix the attacking hydroxide ion at the α position, thus forming copper(I) ions in the product. It is worth noting that ammonium sulfide is an excellent agent for the demetallation of the copper complex. The current approach provides a novel facile route to synthesis of such asymmetrically substituted ligands.

It should be mentioned that the crystalline products of **2**–**4** were all obtained by the slow diffusion of diethyl ether into the dichloromethane solution, resulting in solvated dichloromethane and water molecules in the crystal lattices, which are quite easy to lose. However, TGA analyses show that the thermal decomposition of the desolvated **2**, **3**, or **4** starts at ≈330, 300, and 260 °C, respectively, which indicates high stability.

Crystal structures: There are two crystallographically independent ligands in **1** (Figure 1a, Table 1). Each pair of Hophen ligands, related by a crystallographic twofold axis, is

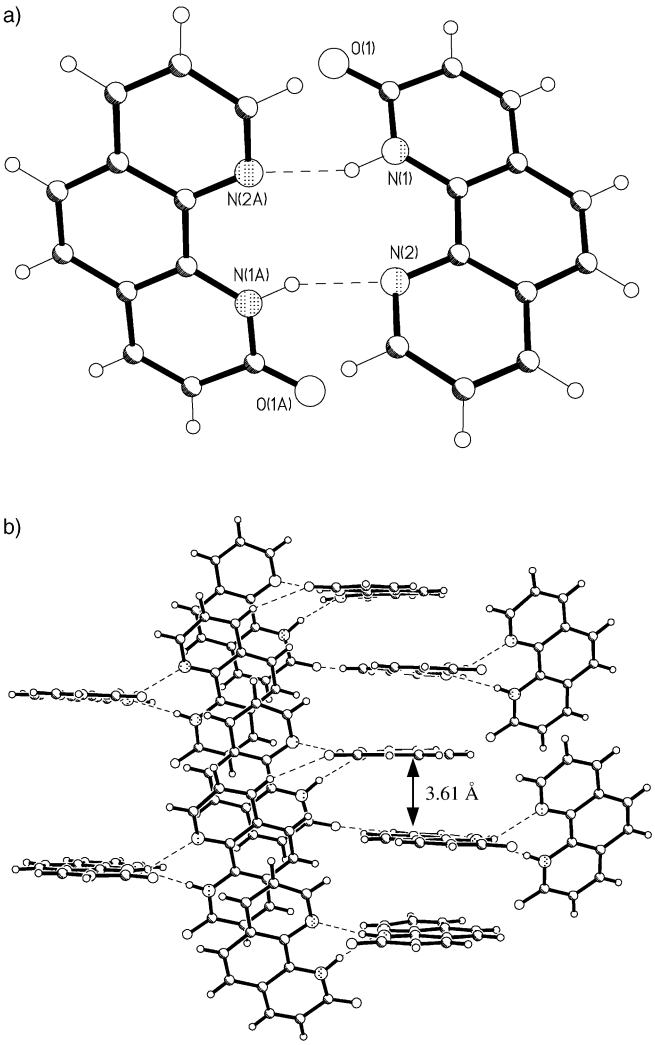

Figure 1. Perspective views showing a) the pair of Hophen ligands and b) two-dimensional supramolecular array viewed along the *a* axis in **1**.

bridged by two N–H···N hydrogen bonds (N···N 3.048(2) or 3.096(2) Å); the dihedral angle between the pair of ligands is ≈61°. The C–O bond length here is 1.233(3) or 1.244(3) Å, which indicates significant double-bond character. Adjacent pairs of Hophen ligands are alternatively stacked through offset aromatic π–π stacking interactions with a face-to-face distance of ≈3.61 Å, and further stabilized by the C–H···O hydrogen bonds[16] between the carbon and oxygen atoms of ophen (C···O 3.45 Å) to furnish two-dimensional layers around the crystallographic (110) planes (Figure 1b). The two-dimensional layers are extended into a three-dimensional

Abstract in Chinese:

本文报道了一个不对称单取代的邻菲咯啉配体，Hophen·0.5H_2O (**1**) (Hophen = 1*H*-邻菲咯啉-2-酮)，及其 d^{10} 金属配合物$[Hg(ophen)_2]\cdot 4H_2O\cdot CH_2Cl_2$ (**2**)，$[Cd_3Cl(ophen)_5]\cdot 1.5H_2O\cdot 2CH_2Cl_2$ (**3**) 和 $[Zn_4O(ophen)_4(OAc)_2]\cdot 4H_2O\cdot 2CH_2Cl_2$ (**4**) 的合成、晶体结构和光物理性质。这些化合物的晶体结构各具特色: 化合物 (**1**) 表现为氢键桥连的二聚体; 化合物 (**2**) 为中性单核分子; 化合物 (**3**) 是通过 ophen 的μ-氧桥连形而的三核结构; (**4**)则含 ophen 的μ-氧基和羧基桥连的 Zn_4O 四核结构。上述配合物的晶体结构中，芳香环π–π堆积作用起重要作用。这些配合物在紫外光激发下，发射强烈的蓝色或绿色荧光。分子轨道计算结果表明，分子轨道的能级与发射光谱基本吻合，不同金属离子可以调控配合物的发光性质。而固态样品所出现的荧光红移现象，则受化合物分子在晶体中芳香环π-π堆积等分子间作用的影响。

Table 1. Crystal data and structure refinements for complexes **1**–**4**.

empirical formula	$C_{12}H_9N_2O_{1.5}$	$C_{25}H_{24}Cl_2HgN_4O_6$	$C_{62}H_{41}Cd_3Cl_5N_{10}O_{6.5}$	$C_{54}H_{46}Cl_4N_8O_{13}Zn_4$
formula weight	205.21	747.97	1544.50	1418.27
crystal system	monoclinic	monoclinic	triclinic	orthorhombic
space group	*P*2/*c* (no. 13)	*C*2/*c* (no. 15)	$P\bar{1}$ (no. 2)	*Fddd* (no. 70)
a [Å]	13.866(4)	9.474(2)	12.604(2)	15.528(2)
b [Å]	8.054(3)	20.074(4)	13.391(2)	22.223(3)
c [Å]	17.781(6)	14.271(3)	19.096(3)	36.005(5)
α [°]	90	90	73.152(3)	90
β [°]	97.956(6)	94.936(3)	83.234(3)	90
γ [°]	90	90	77.644(3)	90
volume [Å^3]	1967(1)	2704.0(9)	3007.7(8)	12424(3)
Z	8	4	2	8
R_{int}	0.0235	0.0379	0.0250	0.0492
R_1 [$I > 2\sigma(I)$]	0.0556	0.0506	0.0335	0.0567
wR_2	0.1898	0.1183	0.0871	0.1926

supramolecular array (see Figure S1 in the Supporting Information) by means of hydrogen bonds between the lattice water molecules and the Hophen oxygen atoms of (O···O 2.868(3) and 2.896(3) Å, Table 2).

Complex **2** is mononuclear. The Hg^{II} ion is located on a twofold axis, and coordinated by four nitrogen atoms from two different ophen ligands, thus completing a distorted tetrahedral geometry (Figure 2a). The Hg–N bond lengths are remarkably different, ranging from 2.091(6) Å (Hg(1)–N(1)) to 2.527(7) Å (Hg(1)–N(2)), concomitant with weak Hg···O contacts (Hg(1)···O(1) 2.978(2) Å) that are well beyond the typical bond lengths (2.38–2.77 Å) documented previously.[17] Similar to the neutral ligand in **1**, the C–O bond length of 1.230(9) Å indicates double-bond character. The dihedral angle between the pair of ophen ligands in **2** is $\approx -87°$ (Figure 2b). Here, the aromatic rings of antiparallel ophen ligands in adjacent molecules face each other with an interligand distance of 3.46 Å, which indicates offset $\pi-\pi$ stacking interactions, thus resulting in two-dimensional layers on the crystallographic (010) planes. The lattice water molecules clathrated among the layers are hydrogen-bonded to each other and to the uncoordinated ophen oxygen atoms (O···O 2.554(9)–3.16(2) Å). Moreover, the C–H···O hydrogen bonds between the dichloromethane carbon atoms with the uncoordinated ophen oxygen atoms (C···O 3.17 Å) were observed. Thus, the adjacent layers are further extended into a three-dimensional supramolecular array (see Figure S2 in the Supporting Information).

Table 2. Selected bond lengths [Å] and angles [°] for **1**–**4**.[a]

				Complex **1**					
O(1)–C(1)	1.233(3)	O(2)–C(13)	1.244(3)	N(1)···N(2A)	3.048(2)	O(2)···O(1W)	2.868(3)	N(3)···N(4b)	3.096(2)
O(1W)···O(2C)	2.896(3)								
				Complex **2**					
Hg(1)–N(1)	2.091(6)	Hg(1)–N(2)	2.527(7)	Hg(1)–N(1A)	2.091(6)	Hg(1)–N(2A)	2.527(7)	O(1)–C(1)	1.230(9)
O(3W)···O(1A)	3.16(2)	O(1W)···O(2WA)	2.554(9)	N(1)-Hg(1)-N(1A)	158.9(4)	N(1)-Hg(1)-N(2A)	122.1(2)	N(1)-Hg(1)-N(2)	72.6(2)
N(1A)-Hg(1)-N(2A)	72.6(2)	N(1A)-Hg(1)-N(2)	122.1(2)	N(2)-Hg(1)-N(2A)	101.2(3)				
				Complex **3**					
Cd(1)–O(3)	2.306(2)	Cd(3)–N(1)	2.275(3)	Cd(1)–-N(3)	2.320(3)	Cd(3)–O(2)	2.332(3)	Cd(1)–O(4)	2.325(3)
Cd(3)–O(5)	2.335(3)	Cd(1)–N(4)	2.379(3)	Cd(3)–N(2)	2.372(3)	Cd(1)–O(1)	2.422(3)	Cd(3)–N(6)	2.409(3)
Cd(1)–Cl(1)	2.540(1)	Cd(2)–O(3)	2.339(2)	Cd(2)–N(7)	2.264(3)	Cd(2)–N(8)	2.366(3)	Cd(2)–N(9)	2.280(3)
Cd(2)–N(10)	2.433(4)	Cd(2)–O(2)	2.301(3)	Cd(3)–N(5)	2.267(3)	O(1)–C(1)	1.272(5)	O(5)–C(49)	1.251(6)
O(2)–C(13)	1.292(5)	O(3)–C(25)	1.299(4)	O(4)–C(37)	1.281(4)	O(1)···O(1W)	2.915(4)	Cl(1)···O(2W)	3.00(1)
O(1W)···O(2W)	3.22(2)	O(3)-Cd(1)-N(3)	104.6(1)	O(2)-Cd(2)-N(8)	87.9(1)	O(3)-Cd(1)-O(4)	84.43(9)	O(3)-Cd(2)-N(8)	170.6(1)
N(3)-Cd(1)-O(4)	87.3(1)	N(7)-Cd(2)-N(10)	91.0(1)	O(3)-Cd(1)-N(4)	175.6(1)	N(9)-Cd(2)-N(10)	70.8(1)	N(3)-Cd(1)-N(4)	71.3(1)
O(2)-Cd(2)-N(10)	175.2(1)	O(4)-Cd(1)-N(4)	93.8(1)	O(3)-Cd(2)-N(10)	92.8(1)	O(3)-Cd(1)-O(1)	91.71(9)	N(8)-Cd(2)-N(10)	96.6(1)
N(3)-Cd(1)-O(1)	83.9(1)	N(5)-Cd(3)-N(1)	114.8(1)	O(4)-Cd(1)-O(1)	169.19(8)	N(5)-Cd(3)-O(2)	106.8(1)	N(4)-Cd(1)-O(1)	89.3(1)
N(1)-Cd(3)-O(2)	87.0(1)	O(3)-Cd(1)-Cl(1)	91.94(7)	N(5)-Cd(3)-O(5)	88.7(1)	N(3)-Cd(1)-Cl(1)	162.98(9)	N(1)-Cd(3)-O(5)	156.0(1)
O(4)-Cd(1)-Cl(1)	98.48(7)	O(2)-Cd(3)-O(5)	81.5(1)	N(4)-Cd(1)-Cl(1)	92.3(1)	N(5)-Cd(3)-N(2)	161.6(1)	O(1)-Cd(1)-Cl(1)	91.73(7)
N(1)-Cd(3)-N(2)	72.1(1)	N(7)-Cd(2)-N(9)	156.0(1)	O(2)-Cd(3)-N(2)	90.2(1)	N(7)-Cd(2)-O(2)	92.1(1)	O(5)-Cd(3)-N(2)	86.9(1)
N(9)-Cd(2)-O(2)	107.2(1)	N(5)-Cd(3)-N(6)	71.5(1)	N(7)-Cd(2)-O(3)	106.5(1)	N(1)-Cd(3)-N(6)	106.1(1)	N(9)-Cd(2)-O(3)	90.4(1)
O(2)-Cd(3)-N(6)	166.3(1)	O(2)-Cd(2)-O(3)	82.78(9)	O(5)-Cd(3)-N(6)	84.9(1)	N(7)-Cd(2)-N(8)	72.4(1)	N(2)-Cd(3)-N(6)	90.4(1)
N(9)-Cd(2)-N(8)	93.6(1)								
				Complex **4**					
Zn(1)···Zn(1A)	3.059(1)	Zn(1)–N(2)	2.130(5)	Zn(1)–O(1)	1.9572(6)	Zn(1)–N(1)	2.190(5)	Zn(1)–O(2A)	2.003(4)
Zn(1)–O(3)	2.124(5)	O(2)–C(1)	1.280(7)	O(1W)···O(1WB)	2.74(2)	O(1)-Zn(1)-O(2A)	113.1(1)	O(3)-Zn(1)-N(2)	84.4(2)
O(1)-Zn(1)-O(3)	100.7(1)	O(1)-Zn(1)-N(1)	94.8(1)	O(2A)-Zn(1)-O(3)	90.6(2)	O(2A)-Zn(1)-N(1)	93.0(2)	O(1)-Zn(1)-N(2)	126.4(1)
O(3)-Zn(1)-N(1)	161.3(2)	O(2A)-Zn(1)-N(2)	120.3(2)	N(2)-Zn(1)-N(1)	78.0(2)				

[a] Symmetry operations: For **1:** A) $-x+1, y, -z+3/2$; B) $-x+2, y, -z+1/2$; C) $x, -y+1, z+1/2$; for **2**: A) $-x, y, -z+1/2$; for **4**: A) $-x+5/4, y, -z+1/4$; B) $-x+1/2, -y+3/2, -z$.

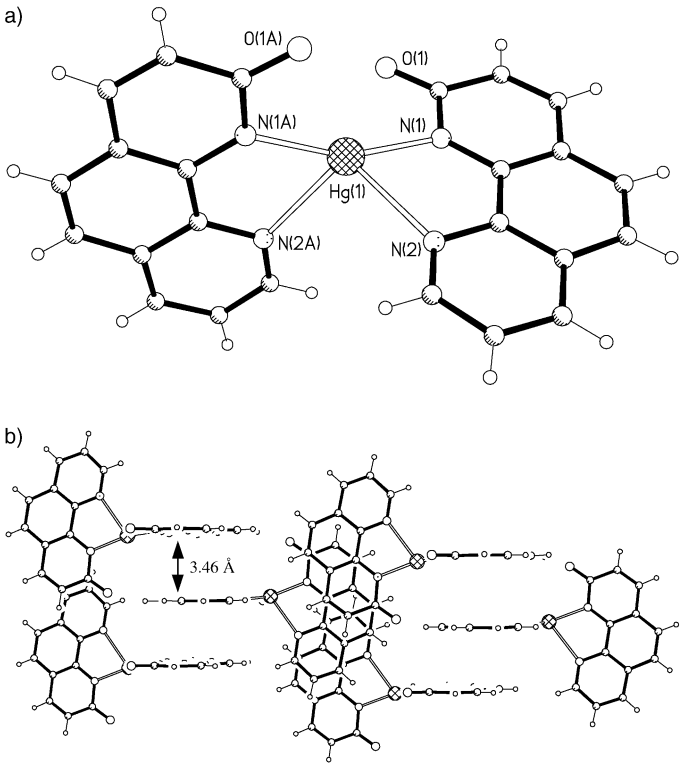

Figure 2. Perspective views showing a) the molecular structure and b) two-dimensional supramolecular arrays viewed along the *c* axis in **2**.

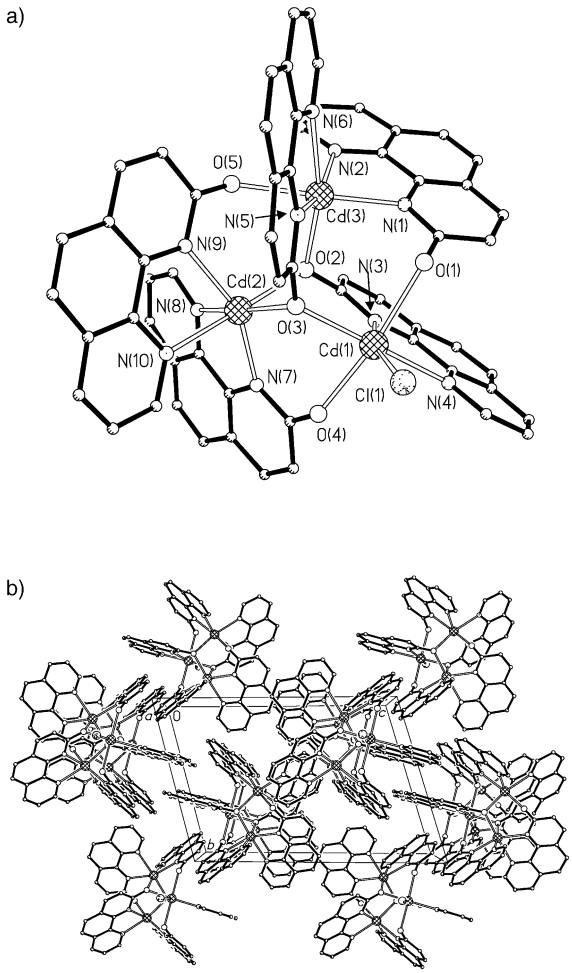

Figure 3. Perspective views showing a) the molecular structure and b) three-dimensional supramolecular array viewed along the *a* axis in **3**. The solvent molecules are omitted for clarity.

As depicted in Figure 3a, the trinuclear molecule in **3** consists of three crystallographically independent Cd^{II} atoms each in distorted octahedron geometry. The Cd(1) and Cd(2) atoms are bridged by an ophen μ-oxygen atom (Cd–O(3) 2.306(2) and 2.339(2) Å; Cd(1)-O(3)-Cd(2) 105.1(1)°) with a metal–metal separation of 3.688(1) Å. The Cd(1) atom is coordinated to a chlorine atom (Cd(1)–Cl(1) 2.540(1) Å), two ophen nitrogen atoms (Cd(1)–N 2.320(3) and 2.379(3) Å) and two oxygen atoms from different ophen ligands (Cd(1)–O 2.325(3) and 2.422(3) Å). While the Cd(2) atom is also coordinated to four nitrogen atoms from two different ophen ligands (Cd(2)–N 2.264(3)–2.433(4) Å), and another ophen μ-oxygen atom (Cd(2)–O(2) 2.301(3) Å), which also forms a bridge to the Cd(3) atom (Cd(3)–O(2) 2.332(2) Å; Cd(2)-O(2)-Cd(3) 102.0(1)°), with a metal–metal separation of 3.600(1) Å. The Cd(3) atom is also coordinated to four nitrogen atoms from two ophen ligands (Cd(3)–N 2.267(3)–2.433(4) Å) and an oxygen atom from a different ophen ligand (Cd(3)–O 2.335(3) Å). It should be noted that the ophen ligands exhibit two different bridging modes. In addition to coordination through both nitrogen sites to chelate one metal ion, each of three ophen ligands can also provide an O-donor to bind another metal ion in a non-coplanar fashion, featuring C–O bond lengths in the range of 1.251(6)–1.281(4) Å; while each of two ophen ligands also provide a μ-O atom to bridge two metal ions with a longer C–O bond length of 1.292(5) or 1.299(4) Å. The supramolecular structure is mainly stabilized by aromatic $\pi-\pi$ stacking interactions. As shown in Figure 3b, the aromatic rings between the adjacent ophen ligands are separated with face-to-face distances of 3.59-3.67 Å in an offset fashion. The lattice water and dichloromethane molecules are clathrated in the interspaces and form donor hydrogen bonds with the ophen oxygen atoms (O···O 2.915(4) Å; C···O 3.109(2) Å) or the chlorine atom (O···Cl(1) 3.01(1) Å; C···Cl(1) 3.542(3) Å).

The most significant structural feature observed in **4** is a tetranuclear Zn_4O core (Figure 4a). The central μ_4-oxo atom, that is bisected by three crystallographic two-fold axes, is surrounded by four Zn^{II} atoms (Zn(1)–O(1) 1.9572(6) Å, Zn-O(1)-Zn 102.81(4)-115.87(4)°) in a tetrahedral geometry, with a non-bonding Zn···Zn distance of 3.059(1) Å. Each Zn^{II} atom is further coordinated by two ophen nitrogen atoms (Zn(1)–N 2.130(3) and 2.190(3) Å), one ophen oxygen atom from another ophen (Zn(1)–O(2) 2.003(4) Å), and one acetate oxygen atom (Zn(1)–O(3) 2.124(5) Å), completing a distorted square-pyramidal geometry, which is different from the common tetrahedral geometry for Zn^{II} atoms in the known Zn_4O complexes.[4–6] Each acetate displays the unique non-coplanar skew–skew μ-bridging mode[18] with Zn-O-C-C torsion angles of $-150.7(2)$°. The ophen ligand uses not only two nitrogen sites but also an O-donor site to bind the Zn^{II} atoms, featuring a C–O bond length of 1.280(7) Å. Face-to-face stacking distances of 3.56 and 3.69 Å are observed between intra-/intermolecular aromatic rings, implying the

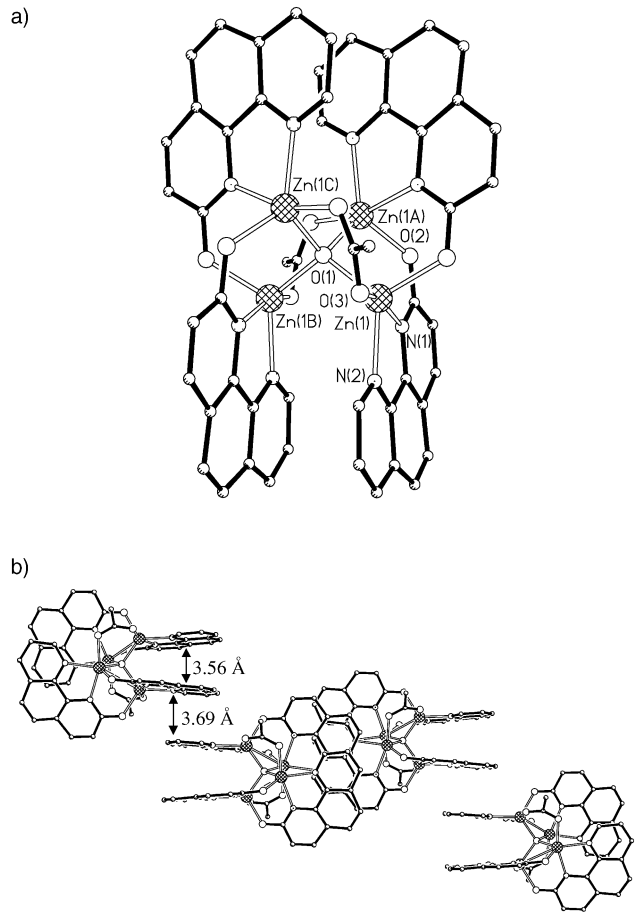

Figure 4. Perspective views showing a) the molecular structure and b) two-dimensional supramolecular array viewed along the *a* axis in **4**.

presence of $\pi-\pi$ stacking interactions (Figure 4b). The partial overlap of the stacked aromatic rings is smaller than those in **2** and **3**, and the atoms are slightly displaced, thus further reducing the $\pi-\pi$ stacking interaction. The lattice water and dichloromethane molecules are located in the interspaces and are hydrogen-bonded to each other (O···O 2.74(2) Å).

Bonding in the aromatic rings: The X-ray crystal structure of the neutral ligand indicates that the proton is bonded to the nitrogen atom instead of the oxygen atom (Figure 1a). The density functional calculations to optimize the geometry for the two possible tautomers (Scheme 1) show that the ketone form (**I**) is more stable by 15.8 kcal mol^{-1} than the hydroxy form (**II**). A similar structural preference can also be found in the pyridone system.[19]

We found that the coordination modes of the ophen ligand are complicated (Scheme 2). The ophen ligand commonly

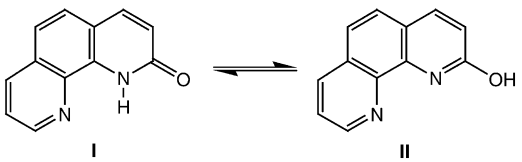

I II

Scheme 1. The possible ketone (**I**) and hydroxy (**II**) tautomers of Hophen.

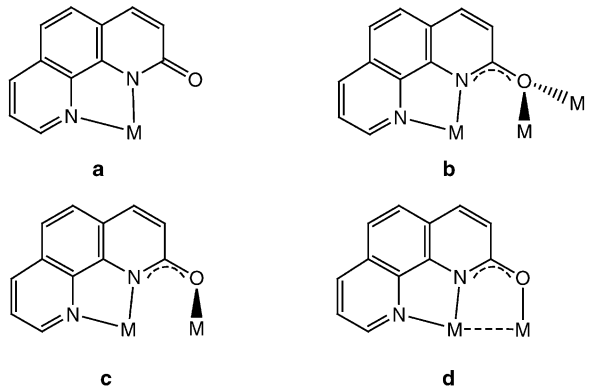

Scheme 2. The complicated coordination modes for ophen. The C–O bond lengths are a) 1.23 Å, b) 1.29–1.30 Å, c) 1.25–1.28 Å, and d) 1.27–1.28 Å.

uses both nitrogen sites to chelate one metal ion, and also provides an O donor to bind another metal ion in a coplanar/non-coplanar fashion, or to provide a μ-O atom to bridge two metal ions. To our knowledge, the typical C–O bond length in aromatic alcohols is ≈1.36 Å,[17, 19] while the typical lengths of C=O bonds in the neutral ligand is ≈1.23 Å. Detailed examination of the geometric data of all known ophen complexes shows that the uncoordinated C–O bond (Scheme 2a) exhibits double-bond character, whereas the coordinated bonds (Scheme 2b–d), have lengths in the range of 1.25 to 1.30 Å, which are slightly lengthened.

Luminescent properties: The neutral ligand emits purple-blue light with an emission maximum at $\lambda = 401$ nm in a dichloromethane solution. Dichloromethane solutions of the metal complexes (concentrations up to ≈10^{-6} M) were also prepared for photoluminescent measurements. The existence of the mononuclear species of **2**, as well as the oligomeric species of **3** and **4**, were confirmed by positive ESI-MS data. The resulting luminescent spectra in solution resemble each other in the peak profiles and all emit in the purple-blue region, despite the different geometry and ligand environment of the complexes (Figure 5). Compared to the emission of the neutral ligand, red shifts of ≈15–30 nm have been observed upon coordination of the metal atoms to the ophen ligands in **2**–**4**.

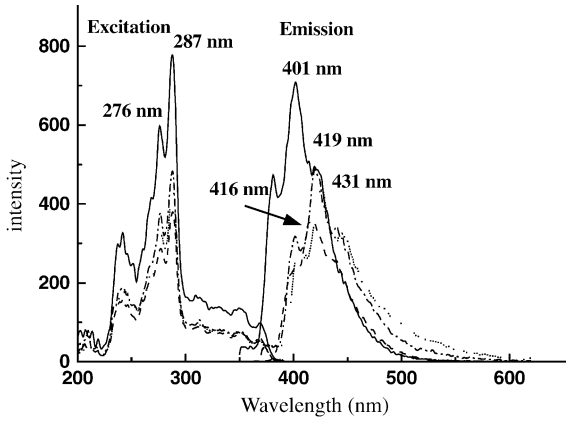

Figure 5. Photoluminescent spectra of **1** (——), **2** (- - - -), **3** (••••), **4** (•–•–) in dichloromethane at room temperature.

To understand the observed luminescent properties of these complexes, we carried out molecular orbital (MO) calculations of the mononuclear Hg^{II} complex and the neutral ligand based on the experimental geometries. As mentioned above, the structural motif of [Hg(ophen)$_2$] in **2** is similar to that in **1**, except the metal connections replacing the N–H···N hydrogen bonds and the difference between the dihedral angles of the pair of ophen ligands. The contour plots (Figure 6) of the relevant HOMOs and LUMOs[20] for Hophen and [Hg(ophen)$_2$], together with the orbital energies, clearly show a significant decrease of the HOMO–LUMO gap of [Hg(ophen)$_2$] compared to that of the neutral ligand. This is consistent with the photoluminescence measurements. In [Hg(ophen)$_2$], the ophen group is more negatively charged owing to the weak electron-accepting nature of Hg^{II} with respect to the lone pairs of electrons from ophen, and the energy of HOMO is thus significantly increased compared to that of Hophen.[3, 7, 21, 22] The LUMO energy, however, is virtually unchanged since the charge effect is much less significant on the unoccupied molecular orbitals. Therefore, a significant reduction in the HOMO–LUMO gap can be seen for [Hg(ophen)$_2$] (0.129 Hartree) compared with Hophen (0.140 Hartree). Calculations of the Cd^{II} and Zn^{II} complexes also show similar decreases in the HOMO–LUMO gaps compared to the neutral ligand with values of 0.113 and 0.127 Hartree for [Cd_3Cl(ophen)$_5$] and [Zn_4O(ophen)$_4$(OAc)$_2$], respectively. It should be noted that the electronegativity values are 2.20 (H), 1.90 (Zn), 1.69 (Cd), and 1.65 (Hg),[21] which implies that the negative charge density for the ophen ligand in the complexes should increase in a regular fashion, resulting in the higher energy of HOMO and the smaller HOMO–LUMO gap. The slight violation of the larger HOMO–LUMO gap of **4** compared to that of **3** can be attributed to the fact that the Zn^{II} ions in the rigid Zn_4O cores of **4** are all five-coordinate and have a greater electron-pulling effect compared to the ophen ligands, concomitant with a larger HOMO–LUMO gap than the six-coordinate Cd^{II} ions in **5** (Table 3 or Figure S3 in the Supporting Information). Moreover, the MO calculations also indicate that the HOMO and LUMO of all d[10] metal complexes are at least mainly associated with the ophen ligands, which may be responsible for the similar emission bands in solution. The HOMO–LUMO gaps that are derived from our calculations match the experimentally measured emission energies very well, and the trend that is derived from the calculations is in accordance with the experimental results (Table 3), although only the ground state was taken into consideration in the calculation, and the maximum deviation (0.7 eV) is found for **1**. In contrast, such deviation may be up to 5 eV.[3, 7] This fact implies that an appropriate selection of the basis set is very important to improve calculations of the MO energies.

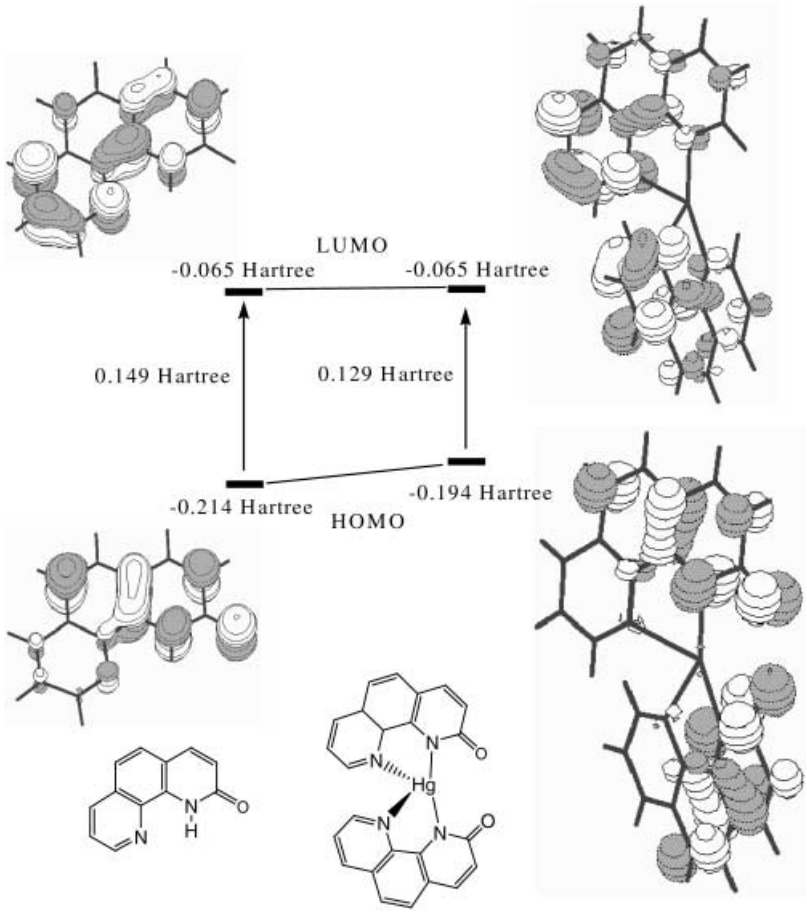

Figure 6. Contour plots of the HOMOs and LUMOs for Hophen and Hg(ophen)$_2$ with the orbital energies.

Table 3. Comparison of the HOMO–LUMO gaps and emission maxima for complexes **1**–**4**.

	Hophen	[Hg(ophen)$_2$]	[Cd_3Cl(ophen)$_5$]	[Zn_4O(ophen)$_4$(OAc)$_2$]
HOMO–LUMO gap [Hartree]	0.140 (3.82 eV)	0.129 (3.52 eV)	0.113 (3.07 eV)	0.127 (3.45 eV)
λ_{max} [nm] (in CH_2Cl_2)	401	416	431	419
λ_{max} [nm] (solid state)	420	544	497	489

The solid-state photoluminescent spectra of **1**–**4** upon excitation at $\lambda = 355$ nm that were recorded at room temperature are depicted in Figure 7, while those recorded at 150 K and 11 K are depicted in Figure S4 in the Supporting Information. The neutral ligand emits a broad band at $\lambda \approx$ 420 nm at room temperature, with two intense emission maxima at $\approx$414 nm and 433 nm at 11 K, which may be

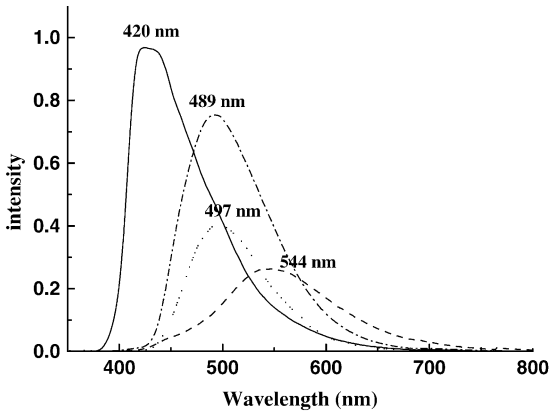

Figure 7. Photoluminescence spectra of **1** (——), **2** (- - - -), **3** (••••), **4** (•–•–) in the solid state at room temperature.

attributed to the slower exchange process between the tautomeric forms of Hophen. Complex **2** shows an emission with a maximum at ≈544 nm, while **3** and **4** exhibit emission maxima at ≈497 and 489 nm in the blue region, respectively. Compared to those of the solution spectra, more significant red shifts were observed. The remarkable red shift of the emission energy from solution to solid is probably caused by the intermolecular π–π interactions of the ophen molecules (or ligands) in the solid state, which effectively decrease the energy gap (Table 3), in accordance with the suggestion that the transverse interactions, such as π–π stacking and hydrogen-bonding interactions, play an essential role in decreasing the HOMO–LUMO gaps.[12, 22, 23]

It should be pointed out that similar to the lifetime of $[Zn_4O(OAc)_6]$ (10 ns),[5] the lifetime of **4** is ≈15 ns, which is significantly longer than those of 2.02, 0.96, and 1.38 ns found for **1**–**3**, respectively (Figure S5 in the Supporting Information). This fact may be ascribed to the presence of the Zn_4O core, as the μ_4-oxo ligand may tighten the whole skeleton and furnish significant intramolecular π–π stacking interactions (Figure 4) between the ophen ligands, thus resulting in much weaker vibrations.[12, 22] In contrast, in a number of complexes featuring Zn_4O cores,[5–7] the HOMO was likely to be a hybrid of the p_π orbitals of the central oxygen atom and another bridging ligand L, whereas the LUMO ($4S_\sigma$) came from the metal 4s orbitals. Thus, besides the possible intraligand π→π* transition of L, the ligand-to-metal change-transfer (LMCT) transition p_π (O^{2-}, L)→$4S_\sigma$ would also exist.[6] However, although the bands are red-shifted, the profile of the emission spectrum of **4** in solution is very similar to that of the neutral ligand, as well as to those of the other metal complexes (Figure 5). Furthermore, cooling the solid sample of **4** to 11 K only led to an enhancement of the emission intensity without any change in the peak profile. Our MO calculation on $[Zn_4O(ophen)_4(OAc)_2]$ shows that the HOMO and LUMO, as well as the orbitals with energies close to the HOMO and LUMO (the energies in the range of −0.198 to −0.040 Hartree) do not have contributions from the zinc atoms and central oxygen atom. In other words, the possible occurrence of LMCT in **4** should be in the higher energy region (>0.158 Hartree). Unfortunately, no other emission bands in the range of 250 nm to 800 nm were found in our further solid-state photoluminescent measurements. Therefore, we can exclude LMCT in **4**.

Conclusion

The Hophen ligand, a monosubstituted 1,10-phenanthroline generated by a facile route, forms a novel class of monomeric or oligomeric d^{10}-metal complexes that have interesting structural features and photoluminescent properties in the blue/green region. The photoluminescent mechanisms have been studied with molecular orbital calculations, which showed that the photoluminescent properties are ligand-based and can be tuned upon ligation to different metal ions. This work demonstrates that the ligand, as well as the metal-tuning approach, may be useful for the preparation of luminescent coordination compounds with the potential for application as new fluorescent materials.

Experimental Section

The reagents and solvents employed were commercially available and used as received without further purification, unless otherwise stated. Methanol and dichloromethane were distilled under a dinitrogen atmosphere. C, H, and N microanalyses were carried out with a Perkin-Elmer 240 elemental analyzer. Thermogravimetric data were collected on a Perkin-Elmer TGS-2 analyzer in flowing nitrogen at a heating rate of 10 °C min^{-1}. FAB-MS and ESI-MS were carried out on a high-resolution Finigan MAT-95 and Finigan MAT LCQ mass spectrometers, respectively. ^{1}H NMR data were recorded on a Bruker Avance 400 DPX spectrometer. FT-IR spectra were recorded in KBr pellets in the range 4000–400 cm^{-1} on a Bio-Rad FTS-7 spectrometer. The emission/excitation spectra were recorded on a Perkin-Elmer LS50B fluorescence spectrophotometer with solution samples. For the solid-state sample, the excitation source was the 325-nm line of a He-Cd laser (Kimmon IK5352R-D). The time-resolved single-photon absorption fluorescence for **1**–**3** was measured with a third harmonic of a mode-locked Nd:YAG laser (Continuum PY61C-10). A duration of 60 ps was used as for excitation source, with a streak camera (Hamamatsu Model C1587, 6 ps resolution) as a recorder, while for **4**, the third harmonics, 355-nm line of an Nd:YAG laser (Quantel Brilliant B) with a duration of 10 ns was used as the excitation light.

Synthesis of Hophen·0.5H$_2$O (1): Crystals of Hophen·0.5H$_2$O were obtained by slow diffusion of diethyl ether into a dichloromethane solution of the pale yellow sample (yield ≈78%; m.p. 159–160 °C; FAB-MS: *m*/*z*: 197 $[M+1]^+$; ^{1}H NMR (400 MHz, TMS, CD_3OD): $\delta = 8.98$ (d, $J = 7.6$ Hz, 1H), 8.36 (d, $J = 7.6$ Hz, 1H), 8.14 (d, $J = 8.2$ Hz, 1H), 7.76 (d, $J = 7.4$ Hz, 1H), 7.70 (d, $J = 7.4$ Hz, 1H), 7.66 (dd, $J = 7.6$, 12 Hz, 1H), 6.82 (d, $J = 8.2$ Hz, 1H)]), which was prepared quantitatively by the demetallation of $[Cu_2(ophen)_2]$[10] in methanol solution by the addition of $(NH_4)_2S$. Elemental analysis calcd (%) for $C_{12}H_9N_2O_{1.5}$ (205.2): C 70.23, H 4.42, N 13.65; found: C 70.20, H 4.40, N 13.64; IR (Nujol): $\tilde{\nu} = 3500$ br m, 1685 m, 1654 vs, 1604 m, 1559 s, 1541 m, 1534 m, 1507 m, 1498 m, 1389 m, 1151 w, 845 m, 688 w, 650 m, 601 w, 522 w, 468 m cm^{-1}.

Synthesis of [Hg(ophen)$_2$]·4H$_2$O·CH$_2$Cl$_2$ (2): Solid Hophen·0.5H$_2$O (0.82 g, 1.0 mmol) was added to a methanol solution (7.5 mL) of $NaOCH_3$ (0.054 g, 1.0 mmol). After the ligand had completely dissolved, $Hg(OAc)_2$ (0.16 g, 0.5 mmol) was added. The mixture was then stirred overnight at room temperature. The pale-yellow product, $Hg(ophen)_2$ (elemental analysis calcd (%) for $C_{24}H_{14}HgN_4O_2$ (591.0): C 48.78, H 2.39, N 9.48; found: C 48.80, H 2.43, N 9.46), was obtained after filtration and heating under reduced pressure at ≈50 °C for 30 min. The crystals of **2** for X-ray crystallography were grown by the slow diffusion of diethyl ether into a dichloromethane solution of $Hg(ophen)_2$. Yield: ≈68%; ESI-MS: *m*/*z*: 591 $[M]^+$; IR (Nujol): $\tilde{\nu} = 3453$ br m, 1654 m, 1549 s, 1560 vs, 1508 m, 1490 s, 1459 vs, 1390 s, 1130 w,1103 w, 846 m, 781 w, 733 m, 697 m, 652 w, 468 w cm^{-1}.

Synthesis of $[Cd_3Cl(ophen)_5]\cdot 1.5H_2O\cdot 2CH_2Cl_2$ (3): Desolvated **3** (elemental analysis calcd (%) for $C_{60}H_{35}Cd_3ClN_{10}O_5$ (1348.7): C 53.43, H 2.62, N 10.39; found: C 53.40, H 2.61, N 10.36) was prepared as for **2** from $CdCl_2$ in place of $Hg(OAc)_2$. Crystals of **3** for X-ray crystallography were also obtained (≈60% yield based on Cd) by the slow diffusion of diethyl ether into a dichloromethane solution of $Cd_3Cl(ophen)_5$. ESI-MS: m/z: 1349 $[M]^+$; IR (Nujol): $\tilde{\nu}$ = 3436 br m, 1654 m, 1617 s,1590 m, 1559 s, 1508 vs, 1482 vs, 1459 vs, 1420 m, 1383 s, 1302 w, 1137 m, 935 w, 848 m, 703 m, 667 w, 638 w, 652 w, 474 m cm^{-1}.

Synthesis of $[Zn_4O(ophen)_4(OAc)_2]\cdot 4H_2O\cdot 2CH_2Cl_2$ (4): Desolvated **4** (elemental analysis calcd (%) for $C_{52}H_{34}N_8O_9Zn_4$ (1176): C 53.09, H 2.91, N 9.52; found: C 53.10, H 2.94, N 9.56) was prepared as for **2** from $Zn(OAc)_2$ in place of $Hg(OAc)_2$. Crystals of **4** for X-ray crystallography were also obtained (≈64% yield based on Zn) by the slow diffusion of diethyl ether into a dichloromethane solution of $Zn_4O(ophen)_4(OAc)_2$. ESI-MS: m/z: 1176 $[M]^+$; IR (Nujol): $\tilde{\nu}$ = 3460 br m, 1624 vs, 1590 s, 1560 vs, 1486 vs, 1388 s, 1308 m, 1139 m, 1082 w,947 w, 845 s, 730 m, 704 m, 661 m, 532 w, 414 w cm^{-1}.

Crystal structure determination: Diffraction intensities for **1**–**4** were collected at 293 K on a Bruker Smart 1000 CCD area-detector diffractometer ($Mo_{K\alpha}$, λ = 0.71073 Å). To prevent crystal collapse because of the loss of solvent, the crystals of the metal complexes were all sealed in glass capillaries. Absorption corrections were applied by using SADABS.[24] The structures were solved with direct methods and refined with a full-matrix least-squares technique with the SHELXS-97 and SHELXL-97 programs, respectively.[25, 26] Anisotropic thermal parameters were applied to all non-hydrogen atoms. The organic hydrogen atoms were generated geometrically (C–H 0.96 Å); the aqua hydrogen atoms were located from difference maps and refined with isotropic temperature factors. Analytical expressions of neutral-atom scattering factors were employed, and anomalous dispersion corrections were incorporated.[27] Crystal data as well as details of data collection and refinements for the complexes are summarized in Table 1. Selected bond lengths and bond angles are listed in Table 2. The drawings were produced with SHELXTL.[28]

CCDC-203893 to CCDC-203896 contain the supplementary crystallographic data for this paper. These data can be obtained free of charge via www.ccdc.cam.ac.uk/conts/retrieving.html (or from the Cambridge Crystallographic Data Centre, 12 Union Road, Cambridge CB2 1EZ, UK; fax: (+44)1223-336-033).

Calculation details: Density functional calculations were performed, employing the Gaussian 98 suite of programs,[29] at the B3LYP level. The basis set used for C, O, N and H atoms was 6–31G while effective core potentials with a LanL2DZ basis set were employed for transition metals. The contour plots of MOs were obtained with the Molden 3.5 graphics program.[30]

Acknowledgement

This work was supported by the National Natural Science Foundation of China (No. 20001008), Ministry of Education of China (No. 01134), Hong Kong Research Grants Council, and The University of Hong Kong.

[1] a) C. H. Chen, J. M. Shi, *Coord. Chem. Rev.* **1998**, *171*, 161–174; b) S. Wang, *Coord. Chem. Rev.* **2001**, *215*, 79–98, and references therein.

[2] a) C. W. Tang, S. A. VanSlyke, *Appl. Phys. Lett.* **1987**, *51*, 913–915; b) C. W. Tang, S. A. VanSlyke, C. H. Chen, *J. Appl. Phys.* **1989**, *65*, 3610–3616; c) Y. Hamada, T. Sano, M. Fujita, T. Fujii, Y. Nishio, K. Shibata, *Jpn. J. Appl. Phys.* **1993**, *32*, L514–L515; d) Y. Hamada, T. Sano, M. Fujita, T. Fujii, Y. Nishio, K. Shibata, *Jpn. J. Appl. Phys.* **1996**, *35*, L1339–L1341; e) J. F. Wang, G. E. Jabbour, E. A. Mash, J. Anderson, Y. Zhang, P. A. Lee, N. R. Armstrong, N. Peyghambarian, B. Kippelen, *Adv. Mater.* **1999**, *11*, 1266–1269.

[3] a) J. Ashenhurst, L. Brancaleon, A. Hassan, W. Liu, H. Schmider, S. Wang, Q. Wu, *Organometallics* **1998**, *17*, 3186–3195; b) J. Ashenhurst, L. Brancaleon, S. Gao, W. Liu, H. Schmider, S. Wang, G. Wu, Q. Wu, *Organometallics* **1998**, *17*, 5334–5341; c) S.-F. Liu, Q. Wu, H. L. Schmider, H. Aziz, N.-X. Hu, Z. Popovic, S. Wang, *J. Am. Chem. Soc.* **2000**, *122*, 3671–3678.

[4] a) C.-F. Lee, K.-F. Chin, S.-M. Peng, C.-M. Che, *J. Chem. Soc. Dalton Trans.* **1993**, 467; b) K.-Y. Ho, W.-Y. Yu, K.-K. Cheung, C.-M. Che, *Chem. Commun.* **1998**, 2491–2492.

[5] a) L. Hiltunen, M. Leskelä, M. Mäkelä, L. Niinistö, *Acta Chem. Scand., Sect. A* **1987**, *41*, 548–555; b) H. Kunkely, A. Vogler, *J. Chem. Soc. Chem. Commun.* **1990**, 1204–1205.

[6] a) J. Tao, M.-L. Tong, J.-X. Shi, X.-M. Chen, S. W. Ng, *Chem. Commun.* **2000**, 2043–2044; b) J. Tao, J.-X. Shi, M.-L. Tong, X.-X. Zhang, X.-M. Chen, *Inorg. Chem.* **2001**, *40*, 6328–6330.

[7] a) W. Y. Yang, H. Schmider, Q. Wu, Y. S. Zhang, S. Wang, *Inorg. Chem.* **2000**, *39*, 2397–2404; b) Q. Wu, J. A. Lavigne, Y. Tao, M. D'Iorio, S. Wang, *Inorg. Chem.* **2000**, *39*, 5248–5254.

[8] a) Y.-G. Ma, C.-M. Che, H.-Y. Chao, X.-M. Zhou, W.-H. Chan, J.-C. Shen, *Adv. Mater.* **1999**, *11*, 852–857; b) M.-L. Tong, X.-M. Chen, B.-H. Ye, L.-N. Ji, *Angew. Chem.* **1999**, *111*, 2376–2379; *Angew. Chem. Int. Ed.* **1999**, *38*, 2237–2240; c) S.-L. Zheng, M.-L. Tong, S.-D. Tan, Y. Wang, J.-X. Shi, Y.-X. Tong, H.-K. Lee, X.-M. Chen, *Organometallics* **2001**, *20*, 5319–5325.

[9] a) V. W.-W. Yam, K. K.-W. Lo, W K.-M. Fung, C.-R. Wang, *Coord. Chem. Rev.* **1998**, *171*, 17–41; b) H. H. Patterson, S. M. Kanan, M. A. Omary, *Coord. Chem. Rev.* **2000**, *208*, 227–241; c) V. W.-W. Yam, C.-L. Chan, C.-K. Li, K. M.-C. Wong, *Coord. Chem. Rev.* **2001**, *216–217*, 173–194, and references therein.

[10] a) X.-M. Zhang, M.-L. Tong, X.-M. Chen, *Angew. Chem.* **2002**, *114*, 1071–1073; *Angew. Chem. Int. Ed.* **2002**, *41*, 1029–1031; b) X.-M. Zhang, M.-L. Tong, M.-L. Gong, H.-K. Lee, L. Luo, K.-F. Li, Y.-X. Tong, X.-M. Chen, *Chem. Eur. J.* **2002**, *8*, 3187–3194.

[11] For example, the copper complex $[Cu_2(ophen)_2]$ can be easily sublimed at 10^{-6} Torr.

[12] H. Yersin, A. Vogler, *Photochemistry and Photophysics of Coordination Compounds*, Springer, Berlin, **1987**.

[13] a) D. V. Scaltrito, D. W. Thompson, J. A. O'Callaghan, G. J. Meyer, *Coord. Chem. Rev.* **2000**, *208*, 243–266; b) L. C. Sun, L. Hammarstrom, B. Åkermark, S. Styring, *Chem. Soc. Rev.* **2001**, *30*, 36–49.

[14] a) E. Z. David, H. C. Francis, *J. Org. Chem.* **1962**, *27*, 3878–3882; b) F. Kröhnke, *Synthesis* **1976**, 1–24; c) J. G. Cordaro, J. K. McCusker, R. G. Bergman, *Chem. Commun.* **2002**, 1496–1497, and refs cited therein.

[15] E. C. Constable, *Metals and Ligand Reactivity*, Wiley-VCH, Weinheim, **1996**.

[16] G. R. Desiraju, T. Steiner, *The Weak Hydrogen Bond in Structural Chemistry and Biology*, Oxford University Press, New York, **1999**.

[17] A. G. Orpen, L. Brammer, F. H. Allen, O. Kennard, D. G. Watson, R. Taylor, *J. Chem. Soc. Perkin Trans. 2* **1989**, S1–S71.

[18] a) Y.-X. Tong, X.-M. Chen, S. W. Ng, *Polyhedron* **1997**, *16*, 3363–3369; b) M.-L. Tong, S.-L. Zheng, X.-M. Chen, *Chem. Eur. J.* **2000**, *6*, 3729–3738.

[19] a) F. A. Cotton, P. E. Fanwick, R. H. Niswander, J. C. Sekutowski, *J. Am. Chem. Soc.* **1978**, *100*, 4725–4732; b) D. P. Kessissoglou, M. L. Kirk, C. A. Bender, M. S. Lah, V. L. Pecoraro, *J. Chem. Soc. Chem. Commun.* **1989**, 84–85.

[20] HOMO, highest occupied molecular orbital; LUMO, lowest unoccupied molecular orbital.

[21] J. A. D. Dean, *Lange's Handbook of Chemistry*, 15th, McGraw-Hill Book Company, Beijing, **1999**.

[22] B. Valeur, *Molecular Fluorescence: Principles and Applications*, Wiley-VCH, Weinheim, **2002**.

[23] a) P. Cassoux, *Science* **2001**, *291*, 263–264; b) H. Tanaka, Y. Okano, H. Kobayashi, W. Suzuki, A. Kobayashi, *Science* **2001**, *291*, 285–287; c) A. Kobayashi, H. Tanaka, H. Kobayashi, *J. Mater. Chem.* **2001**, *11*, 2078–2088.

[24] R. Blessing, *Acta Crystallogr. Sect. A* **1995**, *51*, 33–38.

[25] G. M. Sheldrick, SHELXS-97, Program for Crystal Structure Solution, Göttingen University (Germany), **1997**.

[26] G. M. Sheldrick, SHELXL-97, Program for Crystal Structure Refinement, Göttingen University (Germany), **1997**.

[27] T. Cromer, *International Table for X-Ray Crystallography*, Kluwer Academic Publisher, Dordrecht, **1992**. *Vol C*, Tables 4.2.6.8 and 6.1.1.4.

[28] G. M. Sheldrick, *SHELXTL*, Version 5, Siemens Industrial Automation Inc., Madison, Wisconsin, USA, **1995**.

[29] M. J. Frisch, G. W. Trucks, H. B. Schlegel, G. E. Scuseria, M. A. Robb, J. R. Cheeseman, V. G. Zakrzewski, J. A. Montgomery, Jr., R. E.

Stratmann, J. C. Burant, S. Dapprich, J. M. Millam, A. D. Daniels, K. N. Kudin, M. C. Strain, O. Farkas, J. Tomasi, V. Barone, M. Cossi, R. Cammi, B. Mennucci, C. Pomelli, C. Adamo, S. Clifford, J. Ochterski, G. A. Petersson, P. Y. Ayala, Q. Cui, K. Morokuma, D. K. Malick, A. D. Rabuck, K. Raghavachari, J. B. Foresman, J. Cioslowski, J. V. Ortiz, B. B. Stefanov, G. Liu, A. Liashenko, P. Piskorz, I. Komaromi, R. Gomperts, R. L. D. Martin, J. Fox, T. Keith, M. A. Al-Laham, C. Y. Peng, A. Nanayakkara, C. Gonzalez, M. Challacombe, P. M. W. Gill, B. Johnson, W. Chen, M. W. Wong, J. L. Andres, C. Gonzalez, M. Head-Gordon, E. S. Replogle, J. A. Pople, *Gaussian 98*, Revision A.5, Gaussian, Inc., Pittsburgh, PA, **1998**.

[30] G. Schaftenaar, *Molden*, Version 3.5, CAOS/CAMM Center Nijmegen, Toernooiveld, Nijmegen (The Netherlands), **1999**.

Received: February 18, 2003 [F4855]

